Z. Geomorph. N.F.	Suppl.-Vol. 147	29 – 54	Berlin · Stuttgart	December 2006

Quantitative karst morphology of the Hochschwab plateau, Eastern Alps, Austria

Lukas Plan and Kurt Decker, Wien

with 18 figures and 2 tables

(Supplement: International Karst Atlas Sheet 19)

Summary. The Hochschwab is one of the large karst massifs in the Northern Calcareous Alps, situated in the Austrian province of Styria. As it provides freshwater for the city of Vienna karst morphological field mapping covering 59 km^2 of the plateau area was financed by the Viennese Waterworks. A total of 12,668 karst features – including 7151 dolines – were mapped, attributed and integrated into a GIS. With these data statistical analyses of dolines, dry valleys and corridors were performed and compared to independently derived lithologic and tectonic data. Dolines were analysed with respect to the volume distribution function, spatial density, elevational distribution, host rock lithology, elongation direction and direction of linear arranged features. Additional analyses deal with the direction and inclination of dry valleys and corridors. Glacial overprint proved to be a dominant factor for the occurrence and distribution of several karst features in this high alpine setting. Extremely high densities of rather small dolines are found in areas that suffered from major glacial erosion whereas big features are found on elevated palaeolandscapes. A semi-quantitative classification of the occurrence of dolines, polygenetic poljes, glaciokarstic depressions, cave entrances, Karren and Tertiary clays with respect to the extent of glacial erosion is provided. The dependence of doline occurrence on lithology is not interpretable, as lithologies are not homogenously distributed with respect to glacial erosion, which seems to be the dominating factor. Fault control proved to be the dominant factor for doline elongation and linear arrangement of dolines. Comparison with fault data shows that orientational alignment of karst features mostly parallels sinistral strike-slip faults. Corridors, which are also solutional features, show the same preferred orientation, whereas dry valleys are mainly bound to E-W-directed faults with thick cataclasites that seem to favour erosion.

Zusammenfassung. *Quantitative Karstmorphologie am Hochschwabplateau, Ostalpen, Österreich.* Der in der Steiermark (Österreich) gelegene Hochschwab ist eines der großen Karstmassive der Nördlichen Kalkalpen. Da seine Quellen für die Trinkwasserversorgung von Wien genutzt werden, wurde eine 59 km^2 umfassende karstmorphologische Geländekartierung von den Wiener Wasserwerken finanziert. Dabei wurden 12.668 Karstformen – darunter 7151 Dolinen – kartiert, attributiert und in ein GIS integriert. Diese Daten ermöglichen statistische Analysen von Dolinen, Trockentälern und Karstgassen und den Vergleich mit lithologischen und tektonischen Datensätzen, die unabhängig davon erstellt wurden. Dolinen wurden in Bezug auf ihre Volums-Verteilungsfunktion, räumliche Dichteverteilung, Höhenverteilung, Lithologie, Elongationsrichtung und die Richtung von linear angeordneten Formen untersucht. Von Trockentälern und Karstgassen wurden Richtung und Neigung analysiert. Es wird gezeigt, dass glaziale Überprägung ein dominanter Faktor für das Vorkommen und die Verteilung von Karstformen in diesem hochalpinen Gebiet ist. Bei den Dolinen zeigt sich eine extrem hohe Dichten an kleinen Formen in glazial stark überprägten Gebieten, während große Dolinen auf den hochgelegenen, glazial kaum überprägten Altlandschaften vorherrschend sind. In einer semiquantitativen Klassifizierung wird das Auftreten von Dolinen, polygenetischen Poljen, polygenetischen Hohlformen, Höhleneingängen, Karren und tertiären Lehmen in Abhängigkeit vom Ausmaß der glazialen Überprägung dargestellt. Die

0044-2798/06/0147-0029 $ 6.50

Gesteinsabhängigkeit der Dolinenverteilung kann nicht interpretiert werden, da die Gesteine sehr inhomogen in Bezug auf glaziale Überprägung verteilt sind, und dies der dominierende Faktor ist. Bei den Dolinen beweist die Übereinstimmung der Richtungsmaxima von Elongation und linearer Anordnung, dass Störungen der bedeutendste Einflussfaktor sind. Der Vergleich mit tektonischen Datensätzen zeigt, dass die bevorzugte ENE-Richtung mit der Orientierung sinistraler Blattverschiebungen korreliert. Karstgassen, die ebenfalls Lösungsformen darstellen, weisen dieselbe bevorzugte Richtung auf, während Trockentäler an E-W streichenden Störungen gebunden sind, die aufgrund ihrer mächtigen Kataklasite Erosion begünstigen dürften.

Résumé. Le Hochschwab est l'un des plus grands massifs karstiques des Alpes calcaires du Nord, situé en province de Styrie. C'est l'une des principale source d'eau potable de Vienne. Cette cartographie morphologique couvrant une surface de 59 km2 a été financée par la compagnie viennoise de distribution des eaux. Au total 12 668 objets (dont 7 151 dolines) ont été localisés, caractérisés et intégrés à un Système d'information géographique (SIG). Ces données ont permis d'établir des statistiques sur les dolines, les vallées sèches, les couloirs karstiques, qui ont été ensuite comparées aux données structurales (lithologie et tectonique). La distribution spatiale des dolines prend en compte les paramètres suivants: volume, densité, altitude, lithologie, direction d'allongement et directions des linéaments suivis par les objets morphologiques. L'analyse des vallées sèches et des couloirs intègre l'orientation et la pente.

Le rôle des glaciations est identifié comme un facteur expliquant la distribution et la densité de plusieurs objets morphologiques de cet environnement haut-alpin. Les fortes densités de dolines de tailles réduites se retrouvent dans les zones ayant subi les plus fortes érosions glaciaires, tandis que les formes d'ampleur majeure se localisent sur les hautes paléo-surfaces. Une classification semi-quantitative de la présence de tous ces objets (dolines, poljés polygéniques, dépressions glacio-karstiques, entrées de cavités, lapiaz, et argiles du Tertiaire) a été rapporté à l'extension des glaciers. La dépendance de la présence de dolines selon la lithologie n'est pas interprétable, car les lithologies ne sont pas réparties de manière homogène selon les différentes zones d'érosion glaciaire; ce dernier facteur semble être dominant. Le contrôle des failles est déterminant sur les directions d'allongement des dolines ainsi que sur leur alignement. La comparaison avec les données tectoniques montre que cette direction ENE correspond au second maximum des décrochements sénestres. Les couloirs karstiques, qui sont également des formes de dissolution, se disposent selon la même direction préférentielle, alors que les vallées sèches sont principalement délimitées par des failles E-O fortement bréchifiées, qui semblent concentrer les processus d'érosion.

1 *Introduction*

The Hochschwab karst massif is located in the northern part of Styria (Austria) and is one of the largest karst plateaus of the Northern Calcareous Alps (NCA; Fig 1). The whole mountain range covers an area of 650 km^2 with a system of plateaus having a total area of roughly 120 km^2 with elevations between 1400 to 2277 m.

In contrast to other large karst massifs of the NCA like the Dachstein, Tennengebirge, and Totes Gebirge (e.g., Bauer & Zötl 1971) there are rather few works on karst morphology dealing with the Hochschwab area. Schappelwein (1966) described glacial- and karst features as well as their formation at the easternmost part of the range. The data are depicted in an overview map. He tried to correlate levels of palaeo-surfaces with fore-floods levels. Weißensteiner (1980) provided a 1:50,000 karstmorphological map of the southern Hochschwab range and investigated selected areas speleologically. The report by Fink et al. (2005) contains hydrological data and a brief morphological description of the Hochschwab area of a project finished in 1997.

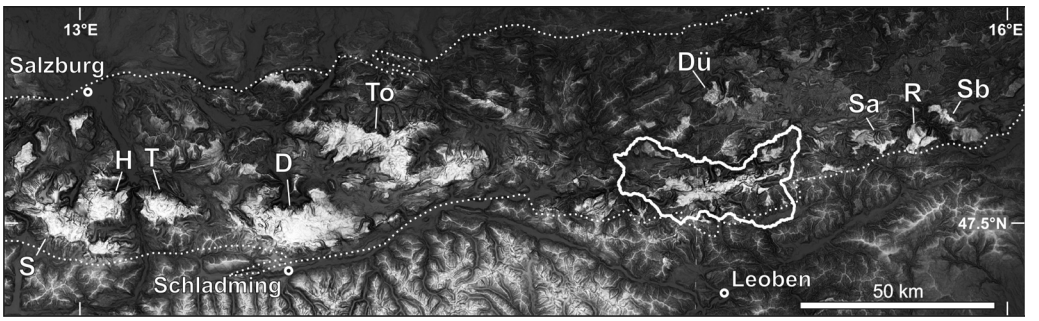

Fig. 1. The Hochschwab mountain range (white polygon) in the Northern Calcareous Alps (NCA). Greyscale of the background map depicts elevation and slop gradient highlighting elevated karst plateaus in white (data base: SRTM); the dotted line delimits the NCA; Karst plateaus: S – Steinernes Meer, H – Hagengebirge, T – Tennengebirge, D – Dachstein, To – Totes Gebirge, Dü – Dürrenstein, Sa – Schneealpe, R – Rax, Sb – Schneeberg.

The detailed karst morphological mapping and quantitative investigation of karst features presented in this paper is motivated by the Vienna Waterworks. Parts of the Hochschwab range are the catchment of springs, which provide roughly 60 % of the water supply for the city of Vienna. For more than 10 years the Hochschwab has been investigated by the interdisciplinary KATER project (KArst waTER research program) initiated by the Vienna Waterworks and co-financed by the EU. The KATER project covers geology, karst morphology, hydrology, silviculture, and ecology (Kuschnig 2001, 2006). Karstology addresses the construction of a database on karst features and morphological parameters influencing the vulnerability of infiltrating waters.

Karst morphological field mapping resulted in a large and detailed dataset including karst morphological maps (58.6 km^2, Supplement 1, 2) and quantitative data on karst features such as the spatial distribution, size and shape parameters as well as phenomenological descriptions (Plan 2002; 2003; Tab. 1). These data were correlated with lithological, tectonical and structural data established by other components of the KATER project (Mandl et al. 2002, Decker & Reiter 2001). Correlations of geological and karst data quantitatively assess the influence of elevation, glaciation, lithology, and tectonic deformation structures on the distribution, shape, and size of karst features. Subsequently these parameters were used to interpret some mechanisms of karst genesis.

2 *Geographic overview*

The Hochschwab plateau system covers a rather narrow (1–10 km wide) strip extending over 34 km from W to E (Fig. 2) with an area of roughly 85 km^2. Several other smaller plateaus are separated from the main part by valleys of mainly glacial origin. The plateau area covers a height range from about 1400 m elevation up to the Hochschwab summit at 2277 m. The whole massif is surrounded by rather deep valleys with floors at 500 to 700 m. The study area comprises the central and eastern main plateau as well as some glacial cirques (Fig. 2).

Table 1. Overview of karst features integrated into the GIS.

type	*no.*	*area [km²]*	*attribute*
dolines (uvalas)	7151	3.91 (6.7 %)	minimum depth
poljes	10	1.06 (1.8 %)	minimum depth
glaciokarstic depr.	38	1.75 (2.9 %)	minimum depth
dry valleys	539	–	narrow/broad (average width >100 m)
corridors	50	–	
Karren fields	764*	–	* for large fields: 1 symbol per ~2500 m²
Karren tables	3	–	description, height of pedestal
registered caves	286	–	data from the cave register
unexplored caves	787		min. estimated depth/length; horizontal (69), vertical (718); notes
possible caves	388	–	horizontal (82), vertical (306)
caves <5 m	1044	–	horizontal (158), vertical (873), arc (13)
streams	726	–	(semi)permanent (72), intermittent (654)
springs	102	–	(semi)permanent (58), intermittent (44)
ponors	111	–	
ponds (Lokva)	179	0.05 (0.1 %)	
Tertiary clays	434	1.41 (2.4 %)	
palaeokarst outcrops	56	–	short description
Sum	*12668*	*58.6 (100 %)**	** total area*

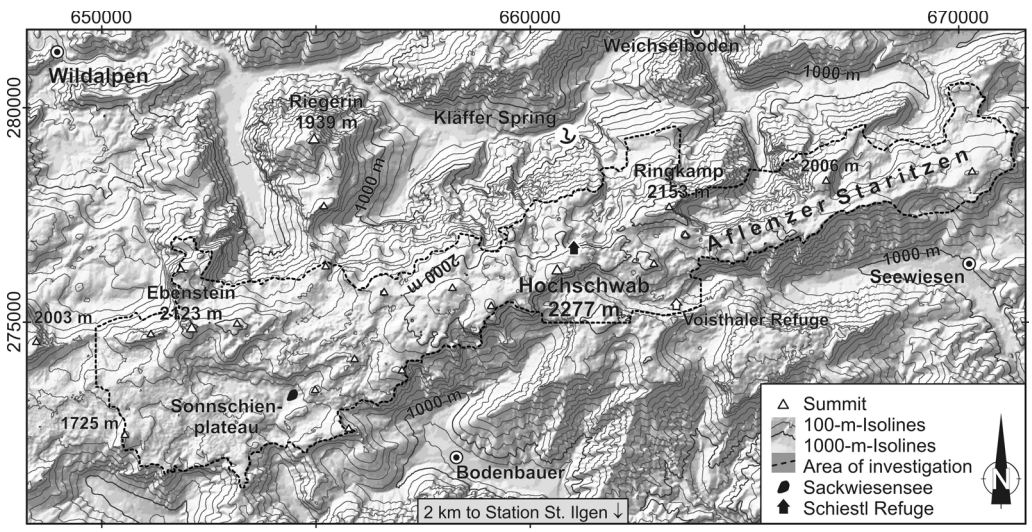

Fig. 2. Map of the Central and eastern Hochschwab range, with the area of investigation (black line). Coordinates: Austrian BMN-grid (in meters).

The alpine climate is chilly with heavy snowy winters and occasionally rainy summers (Fig. 3). The mean temperature at Wildalpen (610 m; Fig. 2) is 5.9 °C (Steiermärkische Landesregierung 2006). At the Schiestl Refuge (2153 m) close to the summit the mean temperature is –0.2 °C. In a N-S-section the precipitation ranges between 1463 mm/a (Wildalpen) and about 2200 mm/a (Schiestl Refuge; Wakonigg 1980) and 1213 mm/a (St. Ilgen, 880 m, S of the plateau). Winter snow piles up to some meters with redeposition by strong, predominantly (south)east directed winds.

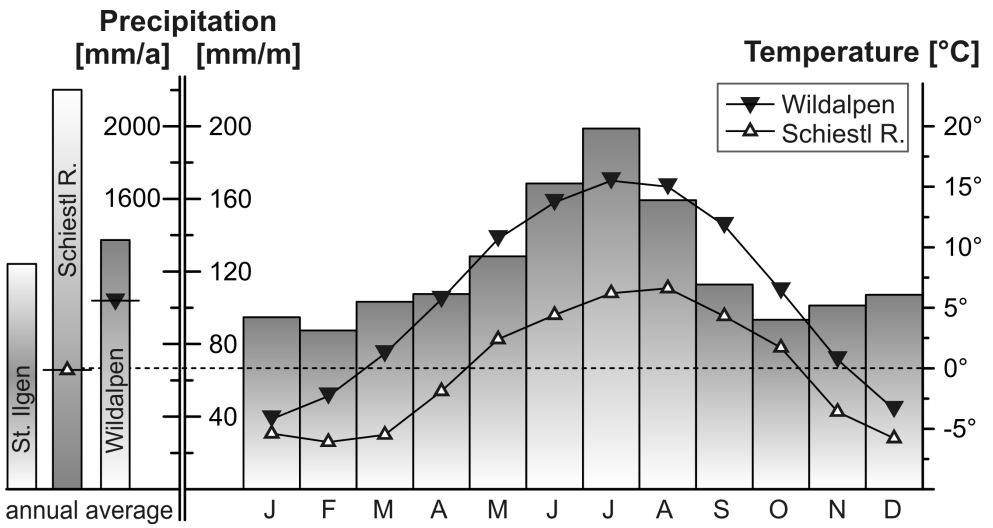

Fig. 3. Mean annual (left) and monthly (right) precipitation (only Wildalpen, 610 m) and temperatures at the stations Wildalpen, Schiestl Refuge (2153 m) and St. Ilgen (880 m; data by Steiermärkische Landesregierung 2006, Wakonigg 1980). See Fig. 2 for locations of the stations.

The entire plateau and most of its slopes shows subsurface drainage. The majority of the study area is part of the catchment of the Kläffer Spring (Fig. 2), one of the biggest springs in the Eastern Alps. It has an average outflow of 4.8 m^3/s (Stadler et al. 2001) and is a typical karst spring, with a dynamic outflow (LQ: 1.0, HQ: 34 m^3/s) and rapid response to rainfall or snowmelt. The spring is located at the northern slope of the Hochschwab massif, close to the Salza River.

The vegetation varies strongly with elevation. Up to ~1600 m, the slopes are covered with forests dominated by spruce and beech trees in the lower and larchs in the higher parts. Above the timberline mugo pines (*Pinus mugo*) occur up to about 1900 m. Grassy vegetation persists up to the summits, where soil coverage has not been washed out due to karstification or erosion. The plateau is uninhabited with only gravel roads for forestry and some tourist facilities. During summer there is limited pasture (some hundred cattle) on the lower plateau areas. Land-use for pasture was more extensive in the past and caused filling of some pits and dolines as well as deforestation.

2.1 *Geology*

2.1.1 *Stratigraphy*

The Hochschwab is part of the NCA (Fig. 1) with the study area located in the Juvavic Mürzalpen Nappe. The stratigraphic sequence exposed in the area (Mandl et al. 2002) comprises up to about 2000 m thick Permian to Upper Triassic sediments with Middle and Upper Triassic carbonates forming a huge karst aquifer devoid of major internal aquitards (Fig. 4). This aquifer extends from the plateau down to the level of the fore-flood north of the range. Sandstone and shale of the Lower Triassic Werfen Formation underlying these calcareous rocks form the only significant aquiclude and non karstic rocks in the area. They are mainly exposed along the southern slope of the massif.

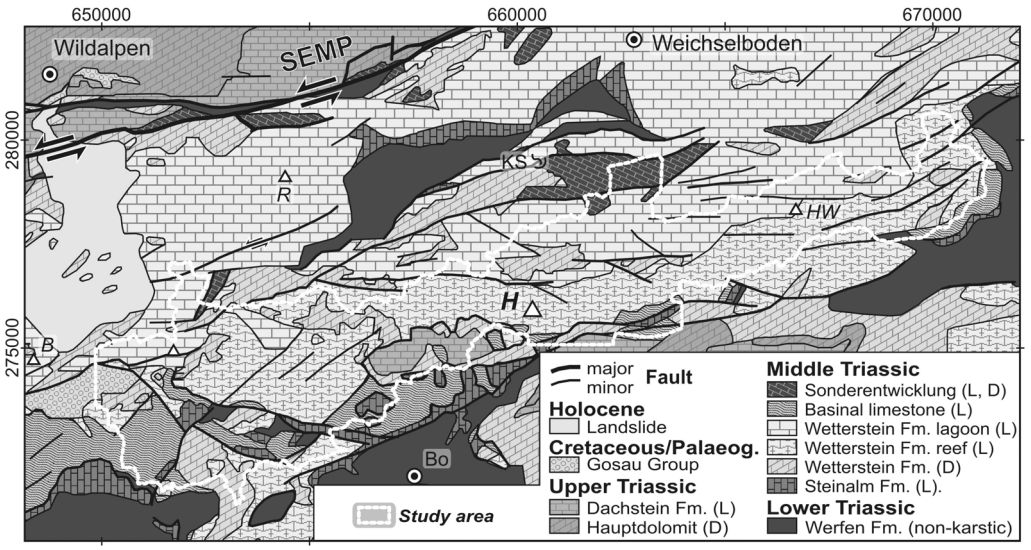

Fig. 4. Simplified geological map modified after Mandl et al. (2002); BMN-grid; H – Hochschwab, HW – Hohe Weichsel, Bo – Bodenbauer, R – Riegerin, E – Ebenstein, B – Brandstein. Abbreviations: L – Limestone; D – Dolostone.

Middle Triassic carbonates of the northern and central part of the study area include up to 1500 m platform limestone and dolostones of the Steinalm and Wetterstein Fm. in lagoonal and reef facies. In both, the lagoonal and reef carbonates bedding planes are not well developed and play actually no role for karstification. Local intra-platform basins with well bedded limestone are referred to as "Sonderentwicklung". To the south, the platform carbonates pass into fore reef, slope and basinal limestones (Wetterstein Fm., slope; Grafensteig Fm.; Sonnschien Fm.) with about 600 m total stratigraphic thickness.

The Upper Triassic includes thin sequences of non karstified marl (North Alpine Raibl Group) of minor local hydrogeological importance and up to several hundred metres thick platform limestone (Dachstein Fm), which only covers the elevated part of the plateau SW and SE of the summit (Fig. 4).

Sediments of the Cretaceous to Palaeocene Gosau Group locally overly the Triassic units with a major unconformity. The group consists of calcareous sandstone, conglomerate, limestone and subordinate marl (W of Sonnschien-Plateau, Fig. 2, 4).

In the Oligocene and Early Miocene crystalline sediments of the Augenstein Fm. were deposited over an Eocene hilly palaeo-karst landscape, which is called "Dachstein Palaeosurface" (Frisch et al. 2000, 2002). These possibly up to ~1 km thick sediments were removed in the Middle Miocene and only single redeposited crystalline pebbles ("Augensteine") are found on the Hochschwab today. However, weathering products of the Augenstein Fm. are common (see 4.10, tertiary clays).

Quaternary sediments have only local significance on the plateau except from the landslide of Wildalpen, which is one of the biggest in the Eastern Alps. It has a volume of about 2.5 km^3 and occurred ~5850 years ago (Fritsch 1993).

2.1.2 *Tectonics and fault mapping*

Tectonic structures govern both groundwater storage and flow in fractured and karstified carbonate rocks to a large extent. This especially applies for faults, which form major discontinuities inside calcareous aquifers. Faults with permeable fault rocks in the fault core or connective fracture networks paralleling faults in narrow damage zones (leaking faults) form preferred groundwater pathways capturing karstification. Other faults with low-permeability fault rocks such as clay gouge may act as impermeable barriers (fault seals) to groundwater flow. The Hochschwab Massif comprises examples for both types of faults. At this background tectonic analyses in the Hochschwab Massif address the identification and characterisation of structures relevant for hydrogeological and karstification processes (Decker & Reiter 2001, Decker et al. 2006). Analyses include regional fault mapping, the establishment of a deformation model and descriptions of the following kinematic groups of faults:

(1) WNW- to NW-striking dextral faults formed during Cretaceous to Eocene folding and thrusting of the NCA. Structures include both fault seals with impermeable cemented cataclasite in dolomite and karstified pathways along faults in limestone. The faults are cut by the younger structures described below and therefore are of limited lateral extent reaching up to about 4 km length.

(2) The by far most important structures in the Hochschwab Massif are ENE-striking sinistral strike-slip faults with E-striking restraining bends. Faults are laterally continuous for tens of kilometres with major sub-parallel faults spaced at distances as small as few hundred meters. By far most of these faults are leaking with permeable cataclasite in dolomite reaching up to 150 m thickness, and karst features such as dolines and caves are aligned with faults in limestone. The structures are part of a crustal-scale shear zone referred to as SEMP (Salzachtal-Ennstal-Mariazell-Puchberg) Fault System (Ratschbacher et al. 1991), which accumulated up to 60 km of lateral displacement in the Oligocene and Miocene (Linzer et al. 2002). The fault delimits the Mürzalpen Nappe to the north (Fig. 4). Miocene sinistral faults, however, do also comprise fault segments with fault seal characteristics. These are related to positive flower structures along restraining bends and contain thick impermeable clay and shale gouge formed by Lower Triassic Werfen Fm., which act as groundwater barriers, and underlie structural poljes. Depending on fault geometry sealing segments may pass into leaking fault segments along the strike of faults.

(3) E- and subordinate W-dipping normal faults of Miocene age form the third group of hydrogeologically important structures. The normal faults crosscut older strike-slip faults. The structures are characterised by lengths of less than 2 km and abundant karstification as shown by frequent fault-aligned caves.

Dating of deformed speleothems in a cave (Hirschgrubenhöhle) located in the central massif proofs neotectonic activity of some of the ENE-striking sinistral faults attributed to the SEMP-System (Plan et al. 2005), which is also supported by local seismicity and GPS-measurements.

3 *Pleistocene glaciation and denudation*

The Hochschwab massif was part of the alpine ice stream network during the Riss and showed local glaciation separated from the ice stream network in the Würm (Van Husen 2000). Big cirques (Fig. 5) cut into the plateau and many of the surrounding valleys are u-shaped. In contrast to these glacial landforms reconstruction of glaciations on the plateau is more difficult as glacial sediments are sparse. Maps of glacier extension for the Würm are provided by Fritsch (1993, NW-part of the range) and Kolmer (1993; NE-part). Both mostly rely on data from the valleys. The map by Schappelwein (1966) shows glacial features on the eastern Hochschwab. A map of glacial morphology (Fig. 6) was compiled from these data and from own observations.

Fig. 5. 1 km wide glacial cirque cutting into the Hochschwab karst plateau (Oberer Ring) with a headwall of 450 m below the Ringkamp summit (2153 m).

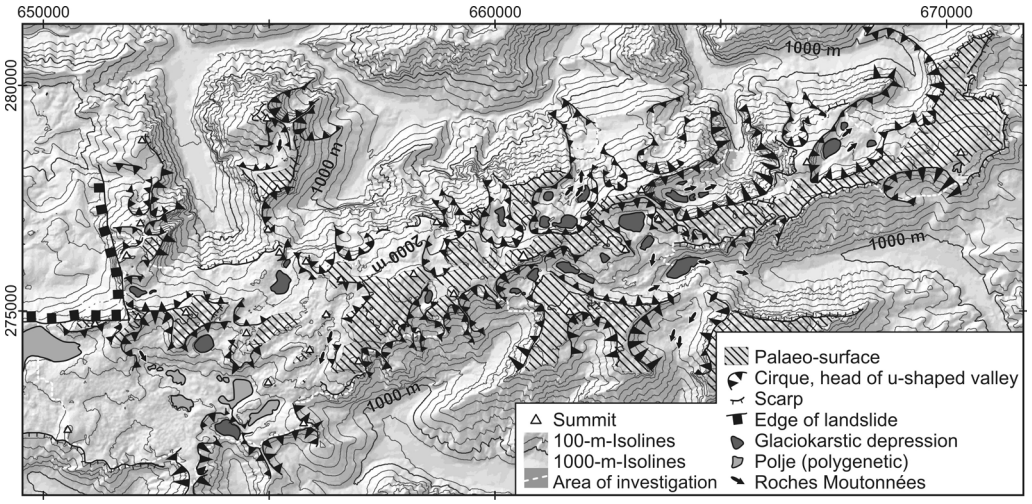

Fig. 6. Palaeosurfaces and glacial morphology (BMN-grid). Basis: Fritsch (1996), Kolmer (1993), Schappelwein (1966), and own observations.

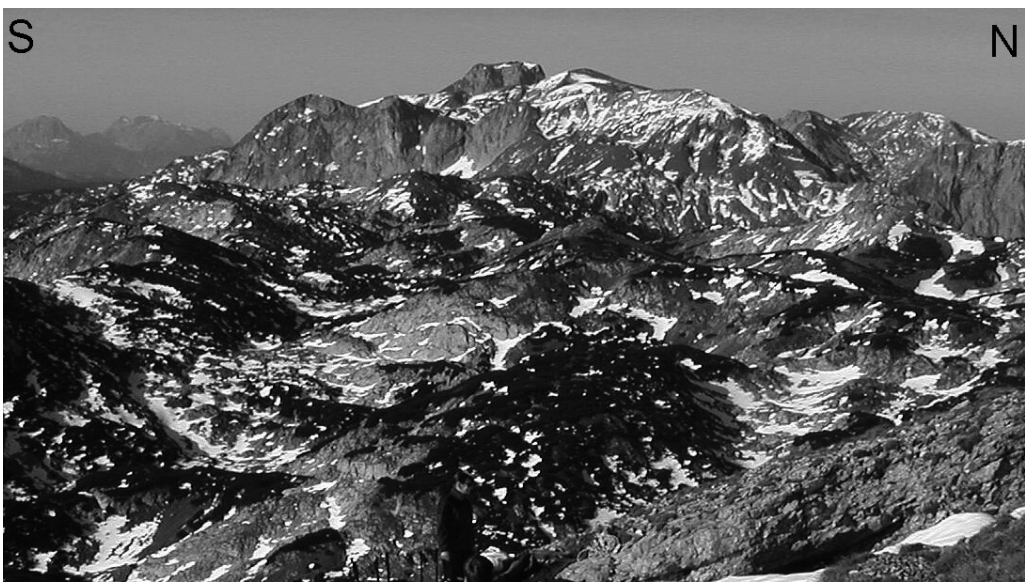

Fig. 7. Central part of the Hochschwab plateau ENE Sonnschien plateau with the Ebenstein summit in the background. The rough topography in the lower part indicates moderate glacial overprint.

(1) Cirques and u-shaped valleys testify major glacial erosion of up to several hundred meters (Fig. 6). The plateau areas show different degrees of glacial overprint. (2) Most of the lower parts of the plateau appear moderately overprinted as shown by rough surfaces (Fig. 7), the absence of Roches Moutonnées, and the local occurrence of moraines. These parts of the plateau are topped by small cirques (e.g., Sonnschien-plateau, Fig. 2). (3) The summits and elevated parts of the plateau either overtopped the massive ice as Nunataker or carried only thin ice shields, which did not reshape the surface significantly. This is shown by rather smooth hilly topography apart from large karst features and the absence of glacial landforms and moraines (Fig. 8). Palaeosurfaces are generally well preserved in altitudes above ~1800 m. Low glacial overprint is also observed in the easternmost part of the plateau (E Aflenzer Staritzen) down to about 1400 m elevation. Preservation of paleosurfaces there is attributed to the lack of elevated accumulation zones.

Fig. 8. Palaeosurface east of the Hochschwab summit (upper right). The hilly surface is characterised by huge dolines. To the left and the right cliffs of cirques cut into the plateau.

3.1 *Karst denudation rates*

Karst denudation rates were investigated by measuring the mass difference of 70 carbonate tablets exposed to natural dissolution for one year. Values range between 13 and 40 µm/a for subcutaneous samples (Plan, 2005). Rates for sub-aerially exposure are about 11 µm/a and agree with data from limestone pedestals (*Karren tables* according to Bögli 1980), which were protected from dissolution by glacial erratics for the past 15 ka. Dissolution calculated from a mass balance, using high-resolution hydrological data from the Kläffer Spring shows a rate of 95 µm/a for a catchment area of 83 km^2.

4 *Field investigation of karst features*

4.1 *Study area, mapping and GIS*

The study area of 58.6 km^2 was investigated by the first author during four summer seasons with a total effort of 115 days (except investigation of caves). Mapping was performed area-wide apart from cliffs and areas densely overgrown by mugo pines which prevent passage. Karst features were drawn in a 1:5000 orthophoto base map that included 10-m-isolines and a coordinate grid for GPS positioning. Beside karst features anthropogenic features like refuges/huts, forestry roads, hiking trails, meadows, cable cars, and gravel pits were mapped. All features were integrated into Arc View GIS 3.2. Table 1 shows the feature types and their attributes. Mapping results are shown in two 1:14,000 maps (Supplement, Sheet 19).

4.2 *Dolines and Uvalas*

Dolines and uvalas were not distinguished as a smooth transition between both forms is observed. Most of the larger features are compound forms with complex geometry, where only the outer limit was mapped. The minimum size for features to be mapped was set to 2 m diameter or 1 m depth. For the discrimination of pit shaped dolines and pits a diameter-depth-ratio of 1:1 was applied. Half dolines were not considered. Depths were measured from the lowest point of the outline down to the lowest point of the depression. Values were visually estimated for small features, measured by laser distance meter and inclinometer for medium sized dolines and barometric altimeter or from the DEM for the largest features. The biggest uvala has an extent of 590 x 320 m (0.10 km^2) and 70 m depth.

Doline morphology is mostly funnel (Fig. 9) but also bowl or pit shaped. Most features seem to be of solutional origin whereas only very few are proven collapse dolines. Several features in the cirques that show the shape of a doline are in fact pits that were truncated by glacial erosion, which can be conducted from speleothems on their bedrock walls. Sometimes accumulation of debris leads to a funnel shape that looks very similar to solutional forms. Most features show a clear structural control by one or more faults.

4.3 *Poljes*

Several structural poljes (classification after Ford & Williams 1989) occur in the SW of the study area. These features are floored by sandstone and shale of the aquitard Werfen Fm., which is uplifted with respect to the surrounding Triassic carbonates at major tectonic faults. The poljes are polygenetic, as glacial erosion modified them to a significant extent (Fig. 6). This is confirmed by a moraine of Würmian age, which formed in one of the poljes. Apart from some micro poljes size ranges from 0.08 to 0.22 km^2. All poljes show a surface drainage system infiltrating into ponors situated on the northern contact between Werfen Fm. and limestones. Lowland moors have developed within some of the poljes and the formation of lakes during snowmelt is reported. The biggest feature lying at the Western margin of the area of investigation ($\sim$1.2 km^2) is geologically different because it is bound to lithologies of the Gosau Group.

Fig. 9. Funnel shaped doline with 170 x 140 m area and a depth of 40 m on palaeo surface in bedded limestone of the Dachstein Fm.

4.4 *Glaciokarstic depressions*

For several big depressions within glacial cirques (Fig. 5, 6) or in u-shaped valleys glacial erosion seems to be the formational process dominating over karstification. Moraines are found in some of the features or below them. Closed glaciokarstic depressions often reach diameters of more than 500 m and depths of up to 60 m. The largest form covers 0.20 km^2. Many of the depressions are elongated as observed in the Altopiani Ampezzani (Dolomites, Italy; Bini et al. 1998). Depressions covered with glacial or periglacial debris host suffusion dolines (Fig. 10) or normal dolines where Quaternary sediments are absent. Open pits are rare.

4.5 *Dry valleys*

Dry valleys are characteristic features of some inclined parts of the plateau. Small dolines and ponors within the valleys show that the modern topography does not allow continuous surface streams. The truncation of some features by the retreat of the plateau margin shows that dry valleys do not form at present. Valleys sometimes start or end in large dolines. Distribution does not show preferential occurrence on certain lithologies nor a preference for palaeosurfaces or glacial landscapes. For some features, or at least segments of them, structural control by faults is obvious. The longest valley is traced for a length of 1.2 km. However, the average length is 127 m with occasionally developed dendritic networks.

Fig. 10. Glaciokarstic depression at the bottom of a cirque (Ochsenreichkar). Karstification moulded suffusion dolines in (peri)glacial deposits. The largest feature on the left has 50 m diameter. A small moraine (M) covers part of the rim of the depression.

4.6 *Corridors*

Long and narrow chasms that seem to be of solutional origin were mapped as corridors. Their floors often show inconsistent inclinations. Most features are fault bound and in some cases corridor walls are formed by fault planes. Only three features WNW of Voisthaler-Refuge are related to vertical bedding planes of limestones of the Grafensteig Fm. They are a few meters broad and range from 25 to 206 m in length.

4.7 *Karren*

Even though Karren features are not as outstanding in the Hochschwab area as on other karst plateaus of the NCA, a great variety of features is observed. In several areas subcutaneous Karren are exposed due to soil retreat. Some show overprints by sub-aerial corrosion. Karren mainly occur in areas with glacial erosion.

4.8 *Caves*

From the area of investigation 286 explored caves (i.e. surveyed, mapped, and documented) are registered in the Austrian Cave Register (Stummer & Plan 2002). However, the Hochschwab plateau has been investigated only punctually. During karst mapping 874 caves were discovered of which 87 have been surveyed meanwhile. Furthermore small (<5 m, which is the limit for registration in Austria) caves and pits were mapped. For 388 features seen in the field or on orthophotos it was not possible to verify them as caves as they are located at cliffs or in densely overgrown mugo pine areas.

A comprehensive characterisation of caves and spatial analyses of the density and distribution of entrances with respect to elevation and lithology is given in Plan (2004). Nearly all caves are pits and sub-vertical canyons with up to 713 m depth that often show deep single pits with up to 451 m. They developed in the vadose zone, which has a thickness of more than 1000 m in the plateau areas. Phreatic cave levels associated with palaeo-valley floors, which make up the huge cave systems in the NCA (Frisch et al. 2002), do not exist in the Hochschwab. A few caves of phreatic origin developed above aquitards such as the Raibl Group. The Hirschgrubenhöhle is the longest phreatic cave with a currently surveyed length of 1.6 km. Initial fissures for speleogenesis are almost exclusively formed by faults. The average density of entrances of registered plus unexplored caves is 18.3 objects per km^2 (Plan 2004). In some areas it increases up to 333 caves per km^2 (see 5.3.2 for statistical methods). High cave densities are especially found in glacially overprinted areas. It is evident that glacial erosion accidentally truncated caves at a previously deeper level exposing speleothems or canyon morphologies at the recent entrances.

4.9 *Hydrological Features*

Springs, streams, and ponors are rare throughout the karst plateau except from poljes. Flow rates are generally well below 1 l/s with only few features in the largest poljes reaching average flow rates of up to few litres per second. Only few (semi)permanent springs persist over exceptionally dry summer periods. In dolostones some seepages are found that feed short minor streams. Non permanent streams are only active after heavy rainfall or snowmelt and mainly form on steep slopes and on dolostone bedrock. During snowmelt much more short surface streams can be observed.

Shallow small ponds with areas below 20 m^2 are mostly restricted to tertiary clays. Only very few ponds in dolines, which are sealed with tertiary clay are deeper than 1 m. The only significant lake (Sackwiesensee) fills a depression within Werfen Fm. in a polje, which was overprinted by glacial erosion

4.10 *Tertiary clays*

Clays sealing the surfaces were mapped in detail as their occurrence and distribution is important for karst morphology. Reddish brown to grey clay with observed thicknesses up to some metres is found on flat areas of the plateau. The outcrops are interpreted as redeposited residual soils of the Miocene Augenstein Fm. (Frisch et al. 2002, Mandl et al. 2002). Pebbles and sand-sized particles dominated by quartz (so-called Augensteine) are only sparsely distributed in the clay. Quartz-rich conglomerates are only known from caves.

Clays in dolines or uvalas create a special morphology called *Karstmulden* (Schappelwein 1966: 119) or *Karstwannen* (Fink 1973: 25). Clay forms flat floors with sharp kinks and secondary dolines at the edges. In glacially overprinted areas only very small occurrences of clay are found in dolines.

5 *Statistical analyses*

Quantitative analyses of the occurrence, distribution and orientation of karst features and their correlation with topography, lithology and tectonic structures use several GIS-based methods of spatial statistics and density analyses along with directional statistics and nearest neighbour analyses (e.g., Denizman 2003, Gao et al. 2005). In the presented approach, karst data are analysed and compared with the independently derived geological and tectonic data not using standard lineament analyses of digital elevation models (DEM) or remote sensing data.

5.1 *Topography: height and aspect distribution in the investigated area*

Height distributions and surface aspects are computed from DEM data with a horizontal resolution of 20 m provided by the Viennese Waterworks. All analysed height values were derived from this DEM. The height distribution and the calculated slope aspects for the study area are shown in Fig. 11. The depicted data are used for comparison and normalisation of the statistical data in the following chapters.

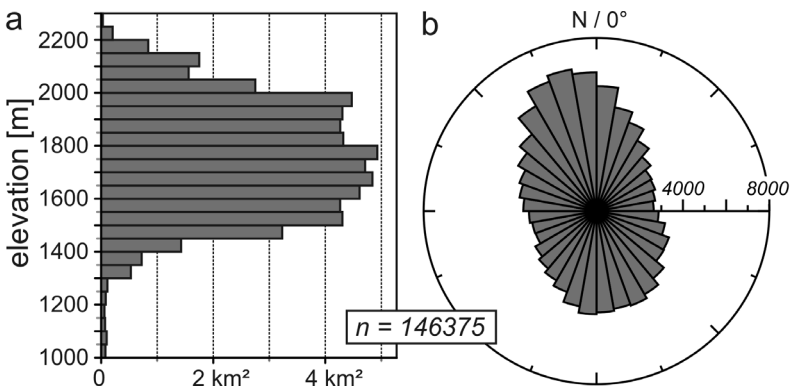

Fig. 11. Histogram of elevation distribution (a) and unidirectional rose diagram (bin size 10°) of surface aspect values of the study area (b).

5.2 *Analysis of fault directions*

GIS-based fault data from the plateaus and the surrounding slopes including the attributes fault kinematics, fault rocks and fault size were used from Decker et al. (2006). The faults are classified according to the deformational model described above with the following main fault systems:

(1) WNW- to NW-striking dextral strike-slip faults, (2) E- and ENE-striking sinistral strike-slip faults of the SEMP-Fault System, and (3) N-striking normal faults. For a statistical directional analysis, which is weighting for fault length, all digitised faults (N = 733) were cut into arbitrary 10 m long segments resulting in a total number of 32,474 segments. Shallow dipping thrust faults were excluded from the data. Directional statistics of the strike directions are plotted in a rose diagram for both: faults with shear sense established in the field, and faults with unknown kinematics (Fig. 17c). The latter dataset shows 4 preferred orientations of faults corresponding to the faults discriminated in the deformation model. With decreasing cumulative fault length directional maxima correspond to E-striking, ENE-striking, N-striking and WNW-striking faults. The dominant E-W-directions are attributed to sinistral strike-slip faults in restraining bends of the SEMP Fault System. The second maximum (~50–65°) represent master faults connecting between restraining bends and / or synthetic Riedl shears within the strike-slip duplexes. The third maximum at around 350° is correlated with normal faults, and the smallest maximum at about 120° derives from dextral strike-slip faults.

5.3 *Analysis of Dolines*

5.3.1 *Doline volume distribution*

Approximate volumes of dolines are calculated for all individual features from surface area and depth assuming cone shape in order to analyse doline size. The simplified procedure leads to errors for the volume of bowl or pit shaped features, which are underestimated, and forms with convex-up slopes, which are overestimated in volume. However, as computed volumes range over 6 orders of magnitude (from 1 to $2.4 \cdot 10^6$ m^3) this simplification is of minor impact on the results.

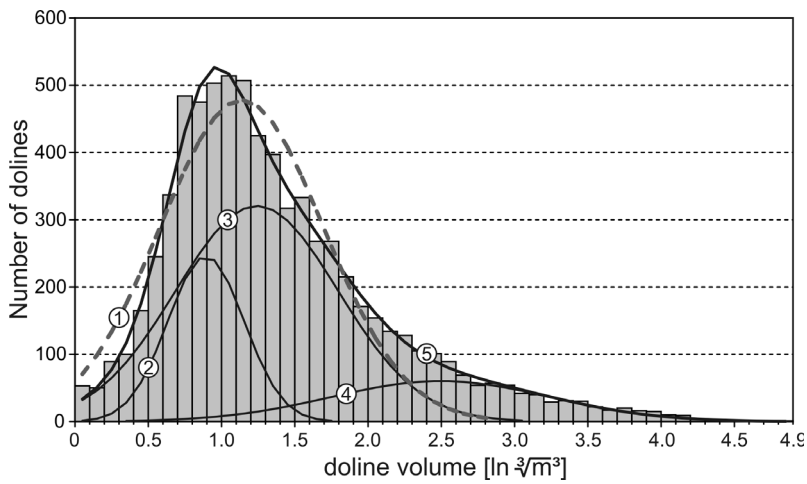

Fig. 12. Histogram of doline volume (grey bars). Numbers of the log-normal distributions curves [1–4] and of the compound curve [5] are explained in the text.

The histogram of doline volumes (in m^3) plotted against the number of dolines shows an extreme skewness of 43.2. Further distribution analyses use the natural logarithm of the cubic root of doline volumes in order to account for the volumetric growth of the structures. Values were classified in a histogram which gives 49 classes for a bin size of 0.1 (Fig. 12).

Doline volume should follow a log-normal distribution as it is a result of some kind of growth (e.g., Limpert et al. 2001). A non linear regression using numerical iteration for such a distribution was calculated but shows rather poor fit (Fig 12; curve [1]). We therefore assume that the total population comprises more than one log-normally distributed subpopulation. Introducing three log-normal distributions [2-4] results in a compound curve [5], that tightly fits the observed distribution with a R^2 of 0.993. The mean values of these distributions (for easier reading expressed as m^3 values) are: [2]: 17 m^3, [3] 48 m^3 and [4]: 2067 m^3.

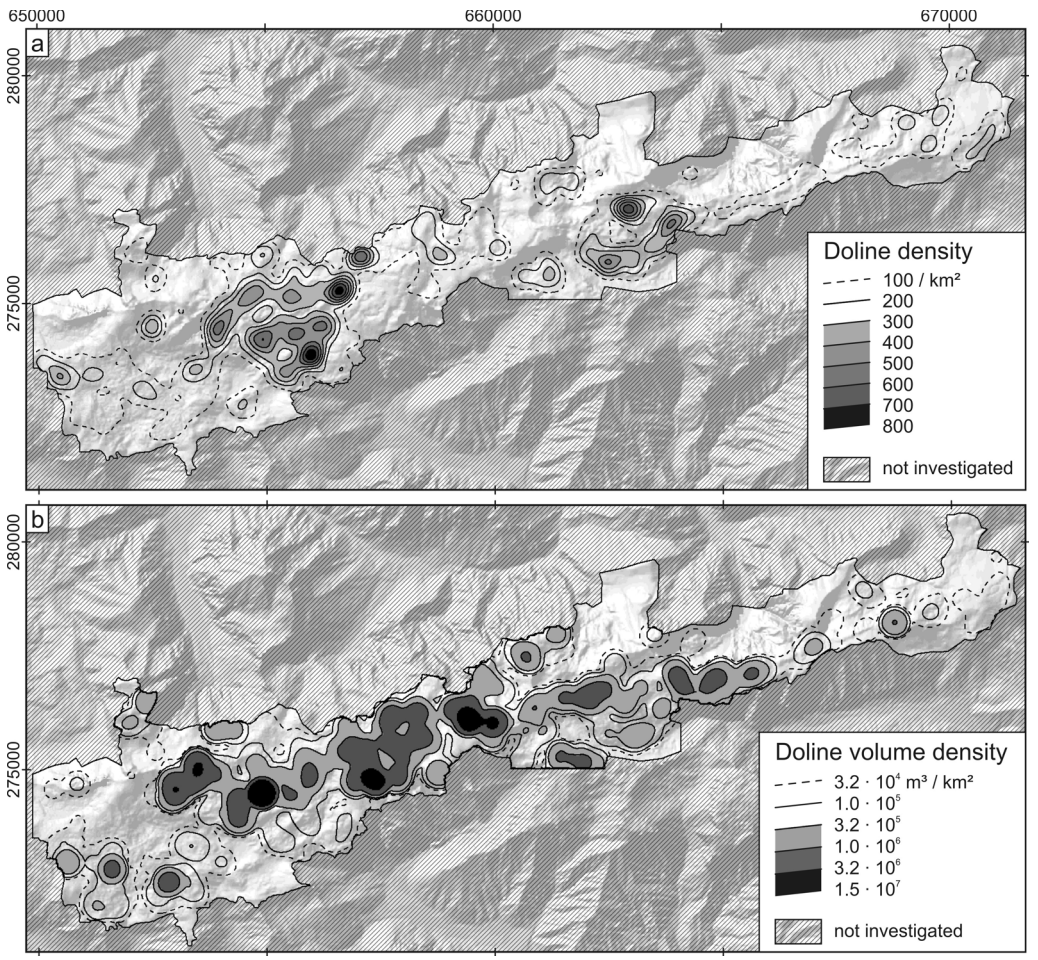

Fig. 13. (a) Isolines of doline density (dolines per km^2). (b) Isolines of doline volume density (m^3 per km^2); BMN-grid.

5.3.2 *Doline density*

The average doline density in the area of investigation is 122 dolines per km^2 with a doline volume density of 3.82 $\cdot 10^5$ m^3/km^2 (total volume of mapped dolines: 2.24 10^7 m^3). The spatial distribution of density was analysed using a search radius of 399 m, which is equivalent to circle of 0.5 km^2. This parameter was chosen in order to provide detailed results without overemphasising the biggest dolines. Smoothed isolines of volume density (Fig. 13a) were computed with a Kernel-Method (Worton 1989). Results for the margins of the investigation area are subjected to minor boundary effects. The results show very heterogeneous distribution of dolines with maximum values reaching 782 dolines per km^2. For a search radius of 564 m, which is equal to 1 km^2, the maximum density is 558 dolines per km^2.

Analyses of the density of doline volume with the same methods (Fig. 13b) show similar heterogeneous distributions with maximum values of 1.5$\cdot 10^7$ m^3/km^2 (7.6 10^6 m^3/km^2 for 1 km^2 search circle). Notably, the maxima of doline density do not coincide with the maxima derived for doline volume density.

5.3.3 *Doline elevation distribution*

Comparison between the frequency of dolines and topographic elevation shows that dolines are most frequent in the interval between 1700 and 1800 m. Results are consistent for both the absolute number of dolines (Fig. 14c) and the number of dolines normalised by the area of the height interval (Fig. 14a). The normalised height distribution of doline volumes shows a rather distinct result with a nearly steady increase of volume with height, which is well approximated by a logarithmic function (Fig. 14b).

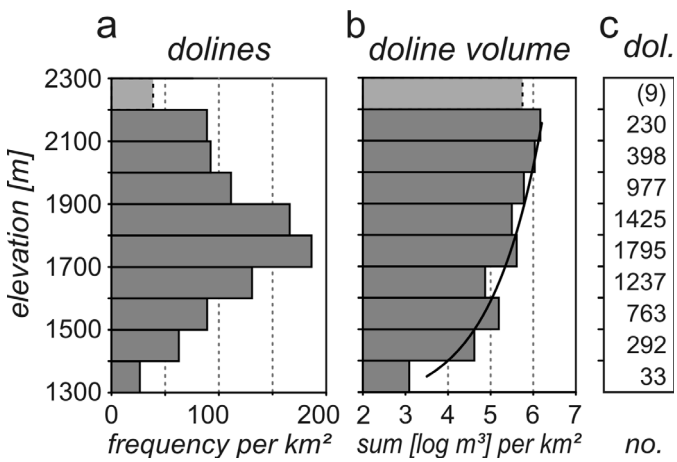

Fig. 14. Histograms of elevation distribution normalised by the area of that height interval of (a) doline frequency and (b) sums of doline volumes. Trendline of best fit function: x = 1.26·ln(y) + 3.42; R^2 = 0.93; highest class was skipped because number of dolines is not representative. (c) Number of dolines in that interval.

In order to analyse the dependence of doline volume on elevation, height histograms were made for 6 logarithmic classes of doline volume with each class comprising one order of magnitude. Fig. 15 plots the number of dolines per class (normalised by the area of the height interval) against elevation. Dolines with less than 10^3 m^3 making up 88 % of the population are most frequent around 1800 m. Medium-sized dolines of the class 10^3 to 10^4 m^3 show an equal distribution of the number of dolines between 1700 and 2300 m. The distribution of big features with 10^4 to 10^6 m^3 (4 % of the total number) is clearly distinct from the distribution of small dolines with maxima above 1900 m, i.e. in the highest parts of the plateau.

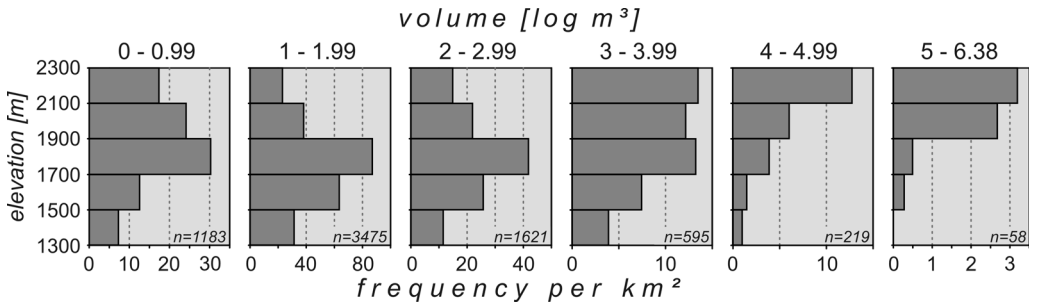

Fig. 15. Doline frequency (normalised by the area of that height interval) plotted against topographic elevation. Data are shown for 6 logarithmic classes of doline volumes.

5.3.4 *Dependence of doline frequency on host rock lithology*

Lithological control on doline occurrence was analysed by correlating doline centroides with host rock lithology. Lithological data derive from the geological map by Mandl et al. (2002). For 608 (8.5 %) features located in Quaternary deposits or in areas covered by Tertiary clay, the bedrock lithology beneath the young cover was interpreted from the geological context. This is especially important for big features as they often host periglacial debris in their centres, which is shown on the geological map. It must be stressed that many dolines developed at the border of two lithologies, e.g. along faults separating distinct lithostratigraphic units. It is assumed that attribution of the centroides to the two adjacent lithologies is random and no systematic error results from this procedure. Fig. 16a shows the distribution of the most important lithostratigraphic units within the area of investigation. Other formations, which make up less than 1 % of the area, were excluded from the analysis. Doline densities respectively doline volume densities normalised by the area of host rock lithology are plotted in Fig. 16b and c.

5.3.5 *Doline elongation direction*

Analyses of doline elongation directions and the orientations of doline arrays were performed to compare preferential orientations of single doline morphologies with the spatial distribution of linearly arranged groups of dolines. Objects with less than 9 m^2 were excluded from elongation

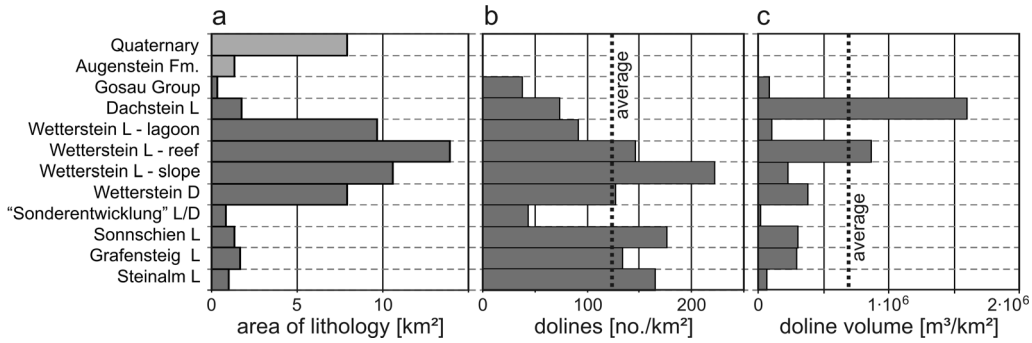

Fig. 16. Histograms of the outcrop area of main lithostratigraphic units (a), doline density (b) and doline volume density (c) (both normalized by the area of host rock lithology for each lithostratigraphic unit). The overall averages of doline density are 122 features per km^2 and 3.82·105 m^3/km^2, respectively. Abbreviations: L – Limestone; D – Dolostone.

analyses as their shape has not been mapped with sufficient precision during 1:5000 field mapping. Nearly circular features were excluded by an algorithm, which compares the actual perimeter to the computed perimeter of a circle with equivalent area. Features with significant elongation are characterised by high ratios of actual perimeter vs. area equivalent perimeter. Empirical testing established a threshold ratio of 1.05 for significantly elongated dolines.

For a total number of 5864 objects exceeding 9 m^2 and perimeter ratios >1.05 orientations of the longest axes were calculated with the algorithm by Jenness (2003). Doline elongations show preferred orientations with a highly significant maximum at 55 to 60° and a second small maximum at 120 to 125° (Fig. 17a).

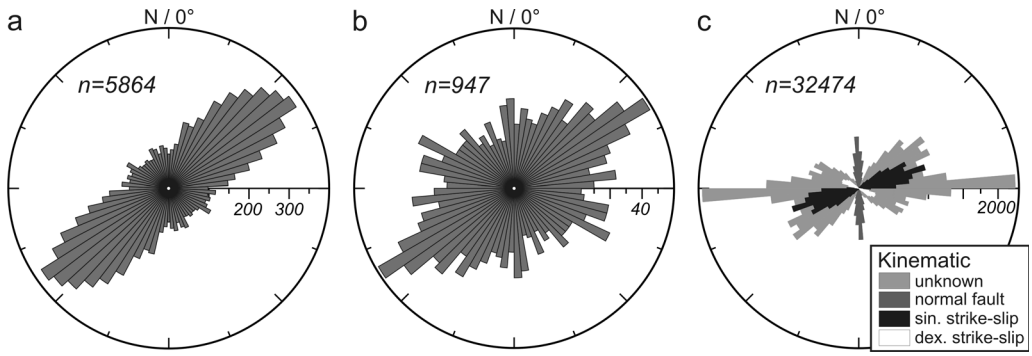

Fig. 17. Symmetric bidirectional rose diagrams (bin size 5°). (a) Azimuth of the longest axes of elongated dolines; (b) Direction of linear arranged dolines (nearest and second nearest neighbour, ±25° tolerance; see text for methodological details); (c): Strike directions of faults weighted for fault length (see 5.2).

5.3.6 *Direction analyses of linear doline arrays*

Preferred orientations of doline arrays are analysed with two approaches. Directions to the first nearest neighbours of doline centroid points (e.g., Gao et al. 2005) determined with the algorithm by Jenness (2004) revealed no significant preferred orientations. The procedure excluded compound forms with perimeters greater than 200 m and nearest neighbours more than 150 m apart from each other.

For a better result an approach comparable to that of Matschinski (1968) was developed. Analyses only include directions defined by three linearly arranged dolines. For each feature (same restrictions as above) the nearest and second nearest neighbours were calculated and only if the directions differ by 180° with a tolerance of ±25° the azimuth between nearest and second nearest centroid was considered (Fig. 17b). It shows a clear maximum at ∼60° and two small maxima at 115 and 180°.

5.4 *Analysis of dry valleys and corridors*

Dry valleys are analysed both with respect to their inclination and direction. Average inclination calculated from the DEM heights of starting and endpoints of the features with a horizontal distance of more than 75 m shows inclinations ranging from 2 to 34°. Inclinations seem to be normally distributed with a median of 18°. 75% of the dry valleys have inclinations between 10 and 26°. A rose diagram summarising the directions of the dry valley segments shows a maximum between 60 and 105° (Fig. 18). For the analysis of corridors features bound to bedding plans were excluded. A clear maximum is visible between 30 and 60° (Fig. 18).

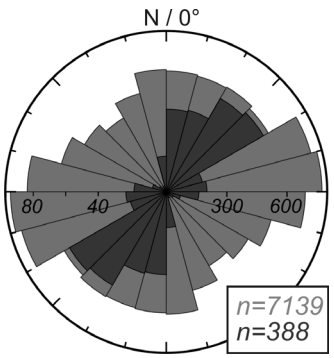

Fig. 18. Directional statistics (bin size 15°) of dry valleys (light grey) and corridors (dark grey) weighted for feature lengths (compare 5.2 for applied methods).

6 *Discussion*

6.1 *Doline distribution and doline volume distribution*

The overall doline density of 122 features per km^2 observed on the Hochschwab plateau is higher than any other value of the compilation by Ford & Williams (1989: 419; highest value: 80) and also much higher than for example on Montello Hill (Ferrarese et al. 1998; value: 43), which is

famous for its high depression density. The cited compilations exclusively contain data from non-alpine and non-glaciated areas. Comparison of the values, however, is problematic as most authors did not consider small features and do not mention the lower size limit recognised by the employed mapping method. Setting the threshold for counting features on Hochschwab plateau to 78.5 m^2 (corresponding to a circular doline with 10 m in diameter) decreases density to 61 dolines per km^2, and setting it to 314 m^2 (20 m diameter) results in a value of 38.

Volume distributions of dolines of the Hochschwab plateau, which do not follow a simple log-normal distribution as it is expected for growth functions (Limpert et al. 2001), strongly suggest a mixed population. The observed distribution can be well modelled as a compound one by inferring more than one log-normally distributed sub-populations. Modelling shows, that for 2 and 3 sub-populations reasonable and very tight fit of synthetic and observed data is achieved (R^2 = 0.975 and 0.993, respectively; Fig. 12).

From this analysis it can only be concluded that the mapped dolines include several log-normally distributed populations. This seems likely when considering cycles of glacial erosion, which caused multiple rejuvenations of doline sub populations in many areas. Straightforward correlation of the introduced log-normal distributions to pre-glacial and post-glacial populations, however, is not possible as the mean values are not comparable to observed data.

6.2 *Factors controlling doline distribution*

For the spatial distribution of dolines and doline volume the degree of glacial erosion seems to be the dominant factor. The spatial distribution of doline density is very inhomogeneous and includes areas where the density is 6 times higher than in average. High density areas correspond to areas of high to moderate glacial modification. Areas with low or zero density mainly coincide with steep slopes, periglacial rectilinear slopes, poljes, and cirques where debris is too thick for the development of suffusion dolines. In contrast to doline density, doline volume distribution has its maxima mainly on palaeosurfaces with low glacial modification. Only in few cases high doline density and high doline volume density is congruent, which means, that there are many relatively big forms. In most cases these are areas of moderate glacial overprinting.

The increase of doline volume with elevation can be interpreted very well with the existence of palaeolandscapes at high altitudes. There, big Pre-Pleistocene dolines are preserved. In lower areas the surface is much younger due to glacial erosion and dolines are generally smaller. Pit shaped and suffusion dolines, which both partly developed from truncated pits, are common.

Analysis of doline volume with respect to lithology shows significant differences. Dachstein limestone shows a volume density four times higher than the average, in Wetterstein limestone in reef-facies it is two times higher. As spatial distribution of the lithologies in dependence on the extent of glacial overprinting is not homogeneous, these results have to be interpreted with care. Dachstein limestone exclusively occurs on palaeolandscapes. Wetterstein reef limestone makes up the Hochschwab summit, big parts of the Aflenzer Staritzen and the palaeolandscape of the Polster. The high volume density for both lithologies therefore is probably an artefact. The long exposure times of the palaeolandscapes seem to obliterate lithological control on karstification.

An alternative explanation for the increase of doline volume with height could be the precipitation rate, which increases with elevation. However, a carbonate dissolution experiment (Plan 2005) showed that dissolution rates do not significantly change with elevation for bare samples. For subcutaneous samples dissolution even decreased with elevation. This is probably related to smaller pCO_2 because of the restricted biological activity at high elevation.

6.3 *Direction analyses of karst features*

Independent analyses of the orientation of both the long axes of elongated dolines and the directions of doline arrays give identical directional maxima around 60° (Fig. 17a, b). This data does not favour the assumption by Schappelwein (1966: 118), who interpreted the dominance of asymmetric E(NE)-W(NW)-elongated dolines as result of the predominant wind direction with preferential snow accumulation and therefore enhanced dissolution in W and WNW edges of this so called *Nivationsdolinen (nivation dolines).* Such effects cannot account for the preferred orientations of doline arrays and, therefore, may not be the dominant factor controlling elongation of individual features. Preferred orientations do not agree with the dominant slope aspect indicating that slope direction has no significant influence on elongation of the majority of individuals.

The identical directional maxima of elongated dolines and linearly arranged dolines suggest structural control on doline formation. Comparison of elongation and array directions with the direction of mapped faults shows that the 60°-maximum parallels the secondary maximum of ENE-striking sinistral strike-slip faults (Fig. 17). Secondary directional maxima of linearly arranged dolines (∼120 and ∼180°) correspond to WNW-striking dextral faults and N-striking normal faults. It is, however, striking that E-striking faults, which form the maximum of the weighted fault orientation distribution, are not imaged by dolines.

Structural control seems to be also important for the orientation of dry valleys and corridors. Directions of corridors (∼50°) show similar maxima as doline elongation and dolines arrays. The direction maxima of dry valleys (∼80°), which do not coincide with the dominant slope direction (∼350°), coincide with the dominant fault directions.

As corridors and dolines primarily are of solutional origin, whereas dry valleys seem to have mainly developed by mechanical erosion, different fault properties may account for their distinct orientation. The E-W-maximum of the fault rose diagram depicts several large faults of the SEMP-Fault-System, which accommodated significant displacement and contain thick cataclasites. Field evidence from several faults shows that these fault rocks facilitate surface erosion and therefore the formation of dry valleys.

7 *Conclusion*

The investigated high alpine karst area of the Hochschwab plateau shows a great variety of karst features. Quantitative analyses with statistical methods of digitised and attributed features and comparison with lithological as well as fault datasets were applied to study several parameters controlling the formation and distribution of the features.

The extreme skewness of the doline volume distribution function and the fact, that it cannot be described satisfactorily with a single log-normal distribution, as it should be the case for growing features, gives rise to the interpretation of a mixed population, which is composed of several log-normally distributed ones. Juvenescence due to glacial erosion is thought to be the reason for the formation of several sub-populations. The average doline density of 122 features per km^2 is very high compared to literature data. Local peak density values are up to 6 times higher. As these correspond to areas of moderate to high glacial erosion this process is interpreted to be the reason for the observed high density.

The dependence of doline distribution on lithology could not be interpreted, as lithologies are not distributed randomly with respect to glacial overprint and elevation. The comparison of karst features with fault data allowed analysing their relationship. Statistics of doline elongation directions and doline arrays show that both azimuths cumulate at around 60°. The dominant factor for the arrangement and shape of dolines are faults striking at this direction. Statistical analyses show that dry valleys are not controlled by dominant slope aspect but most likely also by faults.

Poljes on the Hochschwab range are classified as structural poljes, but show a significant reshaping due to glacial erosion. These polygenetic alpine forms indicate that all hydrologic and morphologic characteristics of a polje can (re)develop within the relatively short period of about 15 ka after the Würmian ice retreat.

Mapping of surface karst features, spatial statistics and the distribution as well as characterisation of caves (Plan 2004) show that the distribution of karst features is highly dependent on the degree of glacial erosion (Table 2).

Table 2. Semi quantitative occurrence of karst features according to the extent of glacial erosion (occurrence: X – rare, XX – moderate, XXX – abundant).

	Glacial erosion		
	insignificant	*moderate*	*extensive*
small dolines ($<10^4$ m^3)	X	XX	XX
big dolines ($>10^4$ m^3)	XXX	XX	X
Poljes		X	XXX
glaciokarstic depressions			XXX
cave entrances	X	XXX	XX
Karren	X	XX	XX
tertiary clays	XXX	XX	

Acknowledgements

The mapping was supported by the Viennese Waterworks (Municipal Department 31) within the KATER I and II project as part of the INTEREG IIIB EU-Programme. We thank especially Gerhard Kuschnig, as project manager, for the financial support. For scientific and linguistic advice we thank Rudolf Pavuza (Dept. of Karst and Caves, Museum of Natural History/Vienna),

Bernhard Grasemann and Stephanie Neuhuber (both Dept. of Geodynamics and Sedimentology, Univ. Vienna). Johann Hohenegger (Dept. of Palaeontology, Univ. Vienna) helped with the non linear regression of doline distribution. In the field, the main author was glad to be partly accompanied by Monika Hölzel, Michael Behm and Alexander Klampfer.

References

Bauer, F. & Zötl, J. (1971): Karst of Austria. – In: Herak, M. & Stringfield, V.T. (Ed.): Karst, Important Karst Regions of the Northern Hemisphere. – Elsevier, Amsterdam.

Bini, A., Meneghel, M. & Sauro, U. (1998): Karst Geomorphology of the Altopiani Ampezzani. – Z. Geomorph. N.F., Suppl.-Bd. **109:** 1–21.

Bögli, A. (1980): Karsthydrology and Physical Speleology. – Springer, Berlin-Heidelberg-New York.

Decker, K. & Reiter, F. (2001): Strukturgeologische Methoden zur Charakterisierung von Karstgrundwasserleitern im Hochschwabmassiv. – In: Mandl, G. (Ed.): Geologische Bundesanstalt Arbeitstagung 2001. – pp. 206–212, Geol. Bundesanst., Wien.

Decker, K., Plan, L. & Reiter, F. (2006): Tectonic assessment of deep Groundwater Pathways in fractured and karstified Aquifers, Hochschwab Massif, Austria. – Proceedings All about Karst and Water, Wien, pp. 138–142.

Denizman, C. (2003): Morphometric and spatial distribution parameters of karstic depressions, Lower Suwannee River Basin, Florida. – J. Cave Karst Stud. **65** (1): 29–35.

Ferrarese, F., Sauro, U. & Tonello, C. (1998): The Montello Plateau. – Z. Geomorph. N.F., Suppl.-Bd. **109:** 41–62.

Fink, M.H. (1973): Der Dürrenstein. – Wiss. Beih. z.Z. Die Höhle 22, Verband Österr. Höhlenforscher, Wien.

Fink, M.H., Pavuza, R. & Stummer, G. (2005): Daten zur Karstverbreitung und Karstgefährdung in den östlichen Kalkhochalpen. – Speldok **16**, Verband Österr. Höhlenforscher, Wien.

Ford, D. & Williams, P. (1989): Karst Geomorphology and Hydrology. – Unwin Hyman, London.

Frisch, W., Székely, B., Kuhlemann, J. & Dunkl, I. (2000): Geomorphological evolution of the Eastern Alps in response to Miocene tectonics. – Z. Geomorph. N.F. **44** (1): 103–138.

Frisch, W., Kuhlemann, J., Dunkl, I., Székely, B., Vennemann, T. & Rettenbacher, A. (2002): Dachstein-Altfläche, Augenstein-Formation und Höhlenentwicklung – die Geschichte der letzten 35 Millionen Jahre in den zentralen Nördlichen Kalkalpen. – Die Höhle **53** (1): 1–36.

Fritsch, A. (1993): Das Quartär der westlichen Hochschwab-Nordabdachung unter Berücksichtigung des Bergsturzes von Wildalpen. – unpubl. diploma thesis, Geol. Inst. Univ. Wien.

Gao, Y., Alexander, E.C. & Barnes, R.J. (2005): Karst database implementation in Minnesota: analysis of sinkhole distribution. – Environment. Geol. **47:** 1083–1098.

Jennes, J. (2003): ArcView extension "Longest Straight Line v. 1.3". – http://arcscripts.esri.com, checked: June 2006.

Jennes, J. (2004): ArcView extension "Nearest Features v. 3.8a". – http://arcscripts.esri.com, checked: June 2006.

Kolmer, C. (1993): Die quartäre Landschaftsentwicklung der östlichen Hochschwab Nordabdachung. – unpubl. diploma thesis, Geol. Inst. Univ. Wien.

Kuschnig, G. (2001): Das Karstforschungsprogramm der Wiener Wasserwerke. – In: Mandl, G. (Ed.): Geologische Bundesanstalt Arbeitstagung 2001. – pp. 213–219, Geol. Bundesanst., Wien.

Kuschnig, G. (2006): KATER II Projekt Web Portal. – www.kater.at, checked: June 2006.

Limpert, E., Stahel, W.A. & Abbt, M. (2001): Log-normal distributions across the sciences: keys and clues. – BioScience **51** (5): 341–352.

Linzer, H.-G., Decker, K., Peresson, H., Dell'Mour, R. & Frisch, W. (2002): Balancing lateral orogenic float of the Eastern Alps. – Tectonophysics **354:** 211–237.

Mandl, G., Bryda, G., Kreuss, O., Moser, M. & Pavlik, W. (2002): Erstellung moderner geologischer Karten als Grundlage für karsthydrogeologische Spezialuntersuchungen im Hochschwabgebiet. – unpubl. final report to the Viennese Waterworks, Geol. Bundesanstalt, Wien.

Matschinski, M. (1968): Alignment of dolines north-west of Lake Constance, Germany. – Geol. Mag. **105:** 56–61.

Plan, L. (2002): Speläologisch-tektonische Untersuchungen der Karstwasserdynamik im Einzugsgebiet der bedeutendsten Quelle der Ostalpen (Kläfferquelle, Hochschwab). – Verband Österr. Höhlenforscher, Wien.

Plan, L. (2003): Tektonisch-karstmorphologische Kartierungen als Grundlage für den Karstwasserschutz im Bereich des Hochschwab-Plateaus. – unpubl. final report, Inst. Geol. Wiss., Wien.

Plan, L. (2004): Speläologische Charakterisierung und Analyse des Hochschwab-Plateaus, Steiermark. – Die Höhle **55** (1-4): 19–33.

Plan, L. (2005): Factors controlling carbonate dissolution rates quantified in a field test in the Austrian Alps. – Geomorphology **68:** 201–212.

Plan, L., Spötl, Ch., Grasemann, B., Decker, K., Offenbecher, K. & Wiesmayr, G. (2005): Seismothems reveal neotectonic activity along the Salzachtal-Ennstal-Fault. – Geophys. Res. Abstr. (EGU) **7**: 04224.

Ratschbacher, L., Frisch, W. & Linzer, H.G. (1991): Lateral extrusion of the eastern Alps, part II: structural analysis. – Tectonics **10:** 257–271.

Schappelwein, K. (1966): Geomorphologische Untersuchungen in den nordöstlichen Steirischen Kalkalpen (Östl. Hochschwab, Zeller Staritzen, Veitschalpe). – Geogr. Jahresber. Österr. **31:** 95–131.

Stadler, H., Strobl, E. & Benischke, R. (2001): Karstwasserdynamik und Karstwasserschutz Hochschwab. – unpubl. report, Joanneum Research, Graz.

Steiermärkische Landesregierung (2006): Aktuelle Niederschlags- und Lufttemperaturwerte. – www.wasserwirtschaft.steiermark.at, checked: May 2006.

Stummer, G. & Plan, L. (2002): Speldok-Austria. Handbuch zum Österreichischen Höhlenverzeichnis. – Speldok **10:** Verband Österr. Höhlenforscher, Wien.

Van Husen, D. (2000): Geological processes during the Quaternary. – Mitt. Österr. Geol. Ges. **92:** 135–156.

Wakonigg, H. (1980): Die Niederschlagsverhältnisse im südlichen Hochschwabgebiet. – In: Fabiani, E., Weißensteiner, V. & Wakonigg, H. (Ed.): Grund- und Karstwasseruntersuchungen im Hochschwabgebiet, Teil II. – pp. 65–141, Amt der Steiermärkischen Landesregierung, Graz.

Weißensteiner, V. (1980): Karstmorphologischen Untersuchungen im südlichen Hochschwab. – In: Fabiani, E., Weißensteiner, V. & Wakonigg, H.: Grund- und Karstwasseruntersuchungen im Hochschwabgebiet, Teil II. – pp. 52–64, Amt der Steiermärkischen Landesregierung, Graz.

Worton, B.J. (1989): Kernel methods for estimating the utilisation distribution in home range studies. – Ecology **70** (1): 164–168.

Addresses of the authors:
Mag. Lukas Plan,
lukas.plan@univie.ac.at
Dr. Kurt Decker,
kurt.decker@univie.ac.at
Department of Geodynamics and Sedimentology, University of Vienna, Althanstr. 14, 2A-344, A-1090 Wien, Austria.